A Novel Robust Design for LPMSM with Minimum Motor Current THD based on Improved Space Vector Modulation Technique

Jawad Faiz
Centre of Excellence on Applied Electromagnetic Systems, School of Electrical and Computer Engineering, College of Engineering, Tehran, Iran
jfaiz@ut.ac.ir

Mehdi Manoochehri and Ghazanfar Shahgholian
Department of Electrical Engineering, Najafabad Branch, Islamic Azad University, Esfahan, Iran.
Mehdi13k@yahoo.com,
Shahgholian47_gh@yahoo.com,

***Abstract*— In this paper a new servo drive system for controlling permanent magnet linear synchronous motor is designed. In the design process, a special space vector modulation technique is applied to obtain a robust system against load disturbance. It also minimizes the current total harmonic distortion in the motor. A desirable and fast drive system with high quality speed tracking is proposed. Simulation results provide a reference frame for software and hardware design which can be implemented in elevators, automations and other linear applications.**

***Keywords*— Robust control, symmetrical space vector modulation, total harmonic distortion, modeling and simulation.**

LIST OF SYMBOLS

i_d, i_q	Rotor dq currents	λ_f	PM flux
u_d, u_q	Rotor dq voltages	FL	Full load
L_d, L_q	Dq inductances	Ω	Angular speed
R	Motor resistance	V	Linear speed
B	Viscous friction coefficient	P=d/dt	Derivative operation

I. INTRODUCTION

Most linear systems are traditionally used rotating electrical motors as well as special transmission devices such as ball rail, roller rail, linear shaft and ball screw systems. The latter devices convert rotating motion into linear motion. Such conversion results in high losses, low efficiency and needs many additional tools. This is the reason for replacing rotational motors by linear motors in most of cases [1-3]. The advantages of linear permanent magnet synchronous motors (LPMSM) include superior thrust density, capability of high performance motion control with fast speed and better accuracy, low thermal losses and high power factor. Therefore, they are being widely used in many automation control fields such as linear actuators, linear elevators in new designed skyscrapers, computer-controlled machining tools, two-dimensional driving devices, robot applications, semiconductor manufacturing equipments and transport propulsions. LPMSM has certain unique features including large air-gap, open-wide slots, pole and interloped PM configurations, flat or tubular configurations and high normal forces in single-sided flat configurations [4-7]. Since conventional gears or ball screws are not used in PMLSM drive systems, load disturbance is easily effected thrust ripples and parameter variations; so designing a trustable and robust control system is the most important task in PMLSM drives [8]. In [9, 10], a control system based on fuzzy logic controller has been designed. Although it provides desirable results, the implementing fuzzy logic controller requires long computations time and experiences. Implementing this control algorithm depends on the applied PC (personal computer) systems.

A field-programmable gate array-based functional link radial basis function network control has been proposed in [11] to control the mover of a PMLSM servo drive system and track periodic reference trajectories. In [12-14], direct thrust force control applied to PMLSM. Although it is a new method having the benefits of direct torque control (DTC) technique, it has high force and current ripples, and variable switching frequency decreases the efficiency. In [15], a modified direct force control (DFC) system based on generic algorithm and new integrator has been modeled. However, it is very complicated to implement and design. In [16, 17], adaptive variable structure has been applied to restraining trust force ripples in application of DFC method. The results reported in the above-mentioned papers are desirable, but the proposed control system is parameter dependent and in most cases it is not easy to obtain its Lyapunov Function.

An analytical technique for estimation of the magnetic field on thrust of LPMSM has been studied for the motor composed of PM Halbach array and air core coil in [18]. Since cogging force in LPMSM is periodic, the high-order harmonic components may be suppressed by proper skewed PMs design while the low-order harmonic components are compensated by a discrete-time linearization observer [19].The force ripples in a double-sided hybrid excited linear flux switching PM has been minimized by a FE-based optimization in [20].

In this paper a control system based on space vector modulation (SVM) technique is designed to achieve a desirable and robust control. Although the method is well-known in rotating electrical, here it is applied to an LPMSM. Digital control technique of SVM is developed to control AC motors. The SVM is generally employed to vary the frequency and adjust the speed of AC motors [21]. Control method of this modulation is based on the selecting effective space voltage vectors during each sampling period, by which an approximate circular rotary magnetic field is obtained. The SVM techniques differ from the carrier based method as such that there are no separate modulators used for each of the three phases. Instead, the reference voltages are given by SVM and the output voltages of the inverter are considered as space vectors. There are eight possible output

978-1-4763-7239-8/15/$31.00 ©2015 IEEE

voltage vectors, six active vectors, and two zero vectors. The reference voltage vector is realized by the sequential switching of active and zero vectors. In other words, the switches are controlled to generate an appropriate voltage waveform as output. This forms the basis of the magnetic flux-linkage tracking pulse width modulation (PWM). The benefits of SVM in comparison with a sinusoidal PWM include not using separate unit for reference signal generation, wider range of linear operation region, increasing modulation index by 91% compared to 78.5% in SPWM, more simple design and implementation, reduction of switching losses possibility in some types of SVM and to implement all kinds of SPWM with SVM [22-24]. It is possible to implement many types of SVM, each type has its own advantages and disadvantages. According to the application and limitations, the appropriate SVM method must be applied. The symmetrical SVM method is applied in this paper to minimize the total harmonic distortion (THD) and increase the efficiency of system in the presence of load disturbances. PMLSM model is presented in section II and principles of symmetrical SVM are explained in section III. In section IV, control system strategy is designed to have a robust and desirable drive. In section V, simulation results are presented and discussed. Section VI concludes the paper.

II. LPMSM Model

To design and simulate a LPMSM drive system, its model must be available. Generally, in this modeling, only fundamental component is considered. Also core saturation, eddy current losses are ignored and damping windings are not included.

There are several mathematical models for LPMSM modeling and dq model is used un [25]. The stator currents (i_a, i_b, i_c) are transformed into the dq currents using 3/2 transformations and then transformed into dq currents in rotor coordinates system. Dq voltages and fluxes equations are as follows:

$$u_d = R i_d + p\lambda_d - \omega_r \lambda_q \quad (1)$$

$$u_q = R i_q + p\lambda_q + \omega_r \lambda_d \quad (2)$$

$$\lambda_d = L_d i_d + \lambda_f \quad (3)$$

$$\lambda_q = L_q i_q \quad (4)$$

Electromotive force (emf) F_M is calculated as follows:

$$F_M = \frac{2\pi}{2\tau}[i_q \lambda_f + (L_d - L_q) i_d i_q] \quad (5)$$

Mechanical motion equation is given by:

$$M\dot{V} = F_M - F_L - BV \quad (6)$$

Generally, it is difficult to model the end-effect using exact mathematical equations due to the limited length of the mover in linear motors. Therefore, finite elements method (FEM) should be applied to analyze the magnetic field and determine the impact of the end-effect in any particular case. In practice, many use multiplying coefficient or function which takes into account the thrust reduction due to the end-effect. The impact of the end-effect on the thrust is reduced with increasing the number of poles of the mover. The value of the coefficient can be determined experimentally [26].

In this paper, the end-effect coefficient is taken to be 0.01. Therefore, 0.99F_M is applied to (6). Figs. 1-3 show the block diagrams of LPMSM mathematical model.

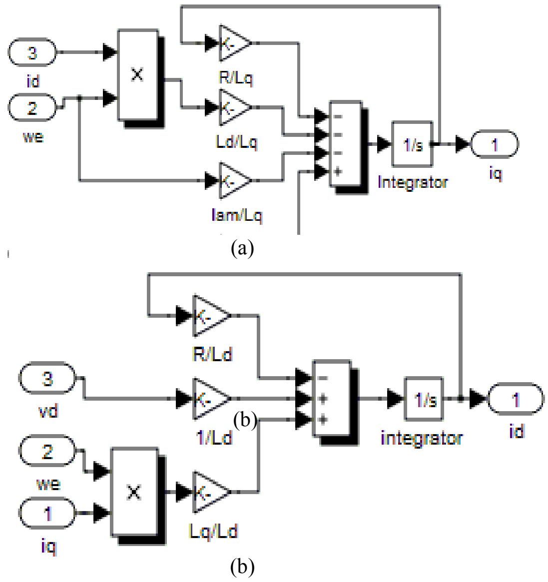

Fig. 1. Deriving (a) i_d and (b) i_q using dq model.

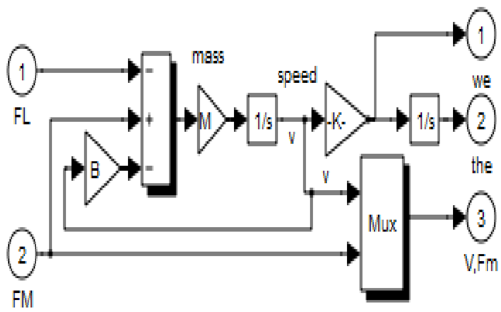

Fig. 2. Mechanical model of PMLSM.

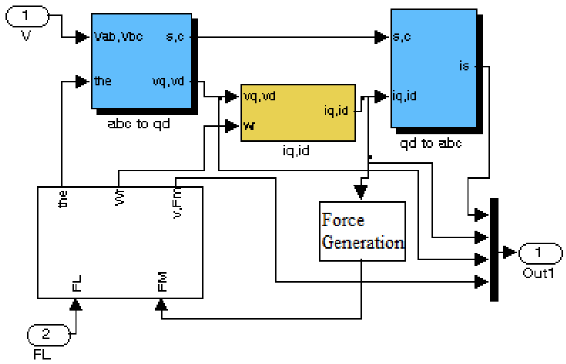

Fig. 3. PMLSM dq model.

III. Principles of Symmetrical SVM

Fig. 4 presents a three-phase inverter supplying the LPMSM. To avoid short circuit, there are 8 possible states for switching and therefore 8 possible vectors for output voltage. These 8 basic voltage vectors consist of 2 zero and 6 nonzero voltages. Switching states for each voltage vector has been given in Table I [23]. The 8 basic voltages are combined to form a desirable reference voltage vector. There are 6 nonzero voltage vectors and so 6 sections in space. So, it is possible to make every reference voltage based on 2 nonzero adjacent voltages and two zero voltages. Fig. 5 shows the basic voltage vectors, reference voltage and 6 sections (Sn). SVM is implemented in three following steps [22].

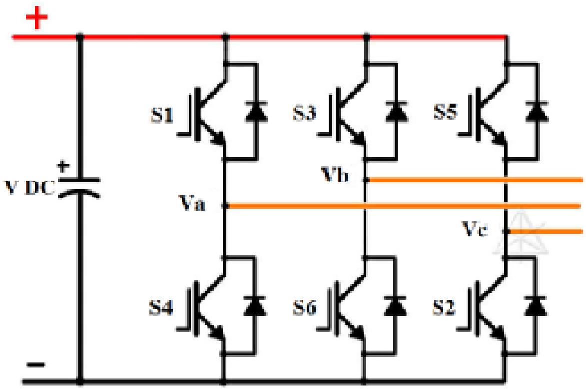

Fig. 4. Three-phase inverter circuit.

TABLE I. SWITCHING STATES IN THREE-PHASE INVERTER

Switching states			Phase voltage (*V_{DC})			Basic voltage vector
S_1	S_3	S_5	V_{an}	V_{bn}	V_{cn}	
0	0	0	0	0	0	V_0
1	0	0	2/3	-1/3	-1/3	V_1
1	1	0	1/3	1/3	-2/3	V_2
0	1	0	-1/3	2/3	-1/3	V_3
0	1	1	-2/3	1/3	1/3	V_4
0	0	1	-1/3	-1/3	2/3	V_5
1	0	1	1/3	-2/3	1/3	V_6
1	1	1	0	0	0	V_7

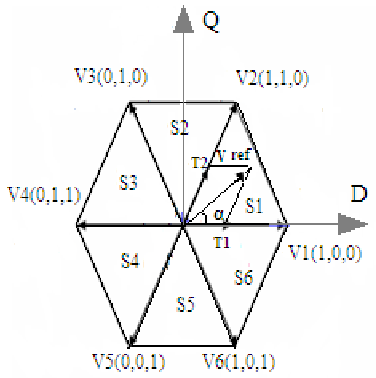

Fig. 5. Basic voltage vectors with their sections.

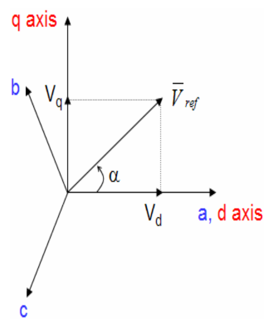

Fig. 6. Reference voltage and its components.

$$\alpha = tan^{-1}\frac{V_q}{V_d} \tag{7}$$

A. Reference Voltage Vector Determination

Determining reference voltage vector needs two dq voltage vector components. Fig. 6 illustrates the relation between dq voltage components and reference voltage (V_{ref}). The amplitude and phase angle (α) of V_{ref} is as follows:

$$\left|V_{ref}\right| = \sqrt{(V_d)^2 + (V_q)^2} \tag{8}$$

In drive systems, determining correct reference voltage is an important part of the control method.

B. Time Durations T_1, T_2, T_0

Fig. 7 presents the time durations of reference voltage located in section 1. Time durations T_1, T_2 and T_0 in n^{th} section are estimated as follows:

$$T_1 = \frac{\sqrt{2}\,T_z\left|V_{ref}\right|}{V_{dc}}[sin(\frac{n\pi}{2} - \alpha)] \tag{9}$$

$$T_2 = \frac{\sqrt{2}\,T_z\left|V_{ref}\right|}{V_{dc}}[sin(\alpha - \frac{n-1}{2}\pi)] \tag{10}$$

$$T_0 = T_z - T_1 - T_2 \tag{11}$$

where $T_z = 1/f_z$.

C. Signals Generation Command

According to the time duration and defined section, the appropriate switching command signal is determined for each sampling time T_z. The command signal for each switch in one leg is the inverse of other one. All SVM types are equal in nonzero voltage vectors ordering [23, 24] and differences are only due to the zero voltage ordering. The ordering differences lead to parameter differences in SVM types. In symmetrical method, the basic voltage vectors applied as such that a symmetric switching algorithm is achieved. This symmetry leads to peak to peak ripple decrement, harmonic content reduction in load current and generated voltages. Also dividing switching period by 7 parts leads to a higher accuracy compared to other SVM types. This switching algorithm for all sections has been shown in Fig. 7. Table II demonstrates this switching algorithm. According to Fig. 7, T_z is divided into 7 parts; to obtain more symmetry, zero voltage vectors have been applied at the first, middle and the end of T_z. In each section, basic voltage vectors are applied due to T_1, T_2, T_0 in order to generate appropriate three-phase voltage.

A desirable SVM method can generates lowest THD, because more harmonics lead to higher losses. Whatever its harmonics order is higher, it is more desirable for filtering which decreases its cost and size. The most important parameter to determine THD is switching algorithm symmetry. Also the number of time division is important [27]. Therefore, symmetrical case including 7 time divisions over one period and maximum symmetry must have lowest THD. Fig. 8 shows three introduced subsystems of SVM structure.

IV. DESIGNING CONTROL SYSTEM

Fig. 9 presents the block diagram of the closed-loop control system for LPMSM, in which the speed error is fed-back to achieve the reference q current. The d reference current is zero. A symmetrical SVM is applied as a modulator similar with that modeled in section III. The generated voltage is used to supply LPMSM. Some transformations are needed during control stage. In this method, current source inverter (CSI) is applied as a control system source. One of the most advantages of CSI is its quick response to the motor sampled current [1]. In this system, PI controllers have been used.

3

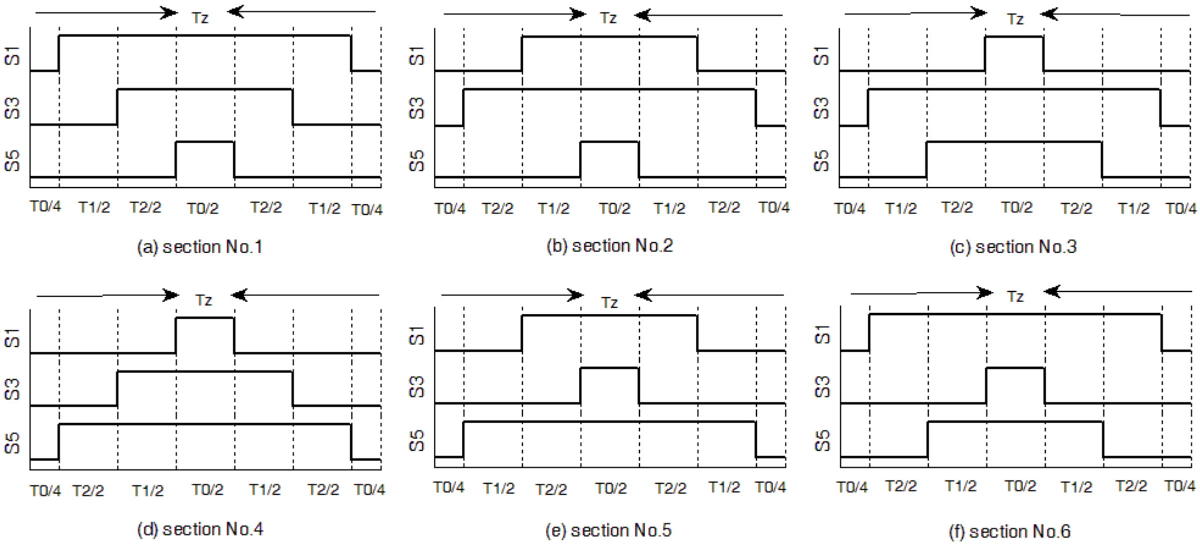

ig. 7. Switching algorithm in symmetrical SVM method.

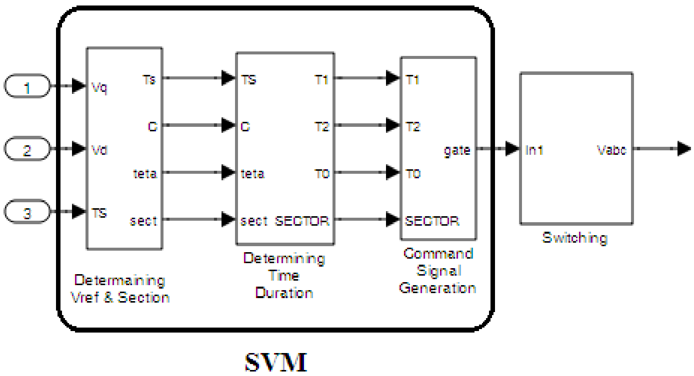

Fig. 8. Block diagram of SVM subsystems.

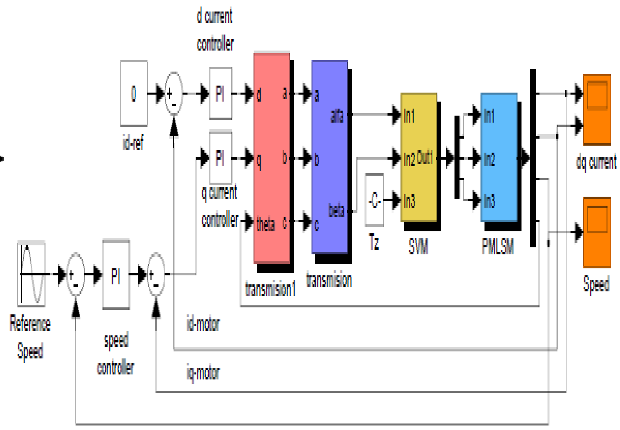

Fig. 9. LPMSM control system based on symmetrical SVM.

IV. Simulation Results

According to Fig. 9, the designed model is used for simulation. In this model, the sampling period of SVM is 400 µs, the DC bus voltage is 250 V, and the carrier frequency of SVM waveform is 20 kHz. The SVM switching algorithm over one sampling period was already shown in Fig. 7. PI controllers are set as given in Table IV. Table III summarizes the LPMSM parameters.

In the following sections the speed tracking, load disturbance effect, three-phase motor current are determined and discussed.

TABLE II. Switching Algorithm for Symmetrical SVM

Sector	Command signal
1	$V_0 \to V_1 \to V_2 \to V_7 \to V_2 \to V_1 \to V_0$ $S1=T_1/2+T_2/2+T_0/2+T_2/2+T_1/2$ $S3=T_2/2+T_0/2+T_2/2$ $S5=T_0/2$
2	$V_0 \to V_3 \to V_2 \to V_7 \to V_2 \to V_3 \to V_0$ $S1= T_2/2+T_0/2+T_2/2$ $S3= T_1/2+T_2/2+T_0/2+T_2/2+T_1/2$ $S5= T_0/2$
3	$V_0 \to V_3 \to V_4 \to V_7 \to V_4 \to V_3 \to V_0$ $S1= T_0/2$ $S3= T_1/2+T_2/2+T_0/2+T_2/2+T_1/2$ $S5= T_2/2+T_0/2+T_2/2$
4	$V_0 \to V_5 \to V_4 \to V_7 \to V_4 \to V_5 \to V_0$ $S1= T_0/2$ $S3= T_2/2+T_0/2+T_2/2$ $S5= T_1/2+T_2/2+T_0/2+T_2/2+T_1/2$
5	$V_0 \to V_5 \to V_6 \to V_7 \to V_6 \to V_5 \to V_0$ $S1= T_2/2+T_0/2+T_2/2$ $S3= T_0/2$ $S5= T_1/2+T_2/2+T_0/2+T_2/2+T_1/2$
6	$V_0 \to V_1 \to V_6 \to V_7 \to V_6 \to V_1 \to V_0$ $S1= T_1/2+T_2/2+T_0/2+T_2/2+T_1/2$ $S3= T_0/2$ $S5= T_2/2+T_0/2+T_2/2$

TABLE III. LPMSM Parameters

Pole pairs	1
Pole Pitch	42 mm
Stator Resistance	2 Ω
dq inductances	2.63 mH
Permanent Magnet Flux	0.17 Wb
Viscous Friction Coefficient	0.001 N.s/m

TABLE IV. PI Parameters Values

PI parameters	Kp	Ki
Speed controller	103	5.1
q axis current controller	10.1	4.9

A. *Speed Tracking*

Fig. 10a shows the speed response to a constant speed reference. The reference speed is 4 m/s and motor starts in t=5 ms under 20 N load which remains constant during 50 ms simulation period. Simulation result shows that the motor starts fast and follows the reference speed with no steady-state error. The rise time is 16.5 ms.

The designed system enables to drive and accelerate the mover in both directions. To show the high quality speed tracking a sinusoidal speed reference as an acceleration motion is applied. Load condition is similar with the previous simulation case. Simulation time is 200 ms. Fig. 10b shows the simulation result in which the motor speed follows the sinusoidal reference speed with a high accuracy, without any steady-state error and a very little lag time

B. Load Changing and Load Disturbances Effect

To investigate the robustness of the control system against load changing and load disturbances two cases are simulated. In the first case, a triangular waveform applied as a variable load. The maximum and minimum loads are 20 N and 0 N respectively. The signal period is 100 ms, reference speed period 4 ms and simulation time 200 ms. Fig. 11 demonstrates that the load change has no impact on the motor speed and remains constant over no-load and

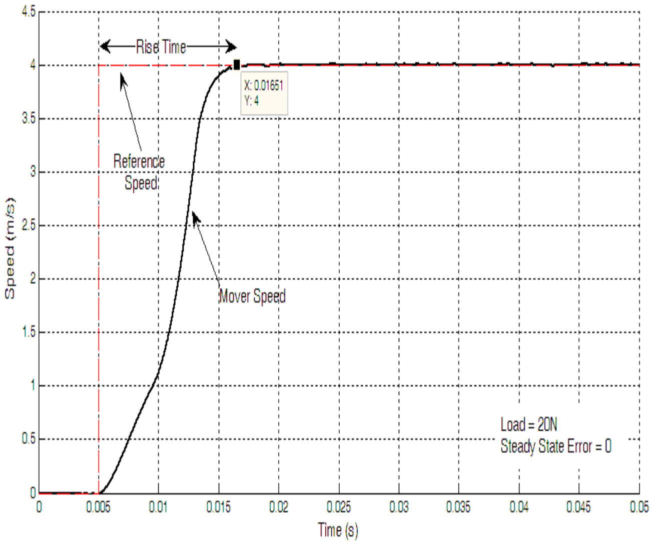

(a)

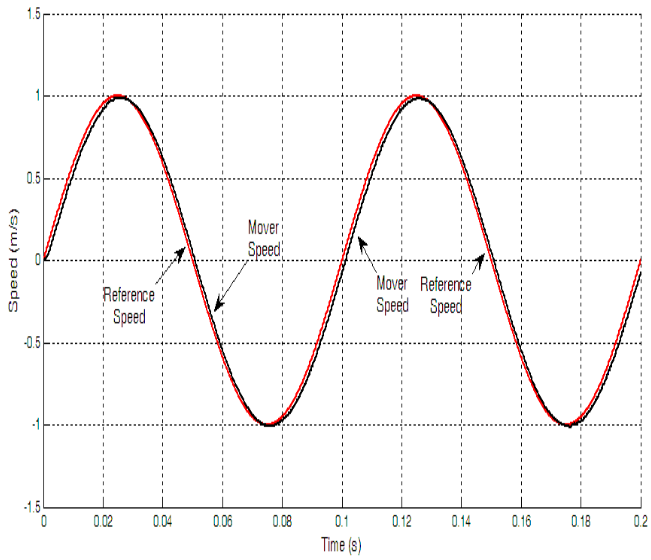

(b)

Fig. 10. Speed tracking by applying: (a) a constant and (b) sinusoidal speed reference.

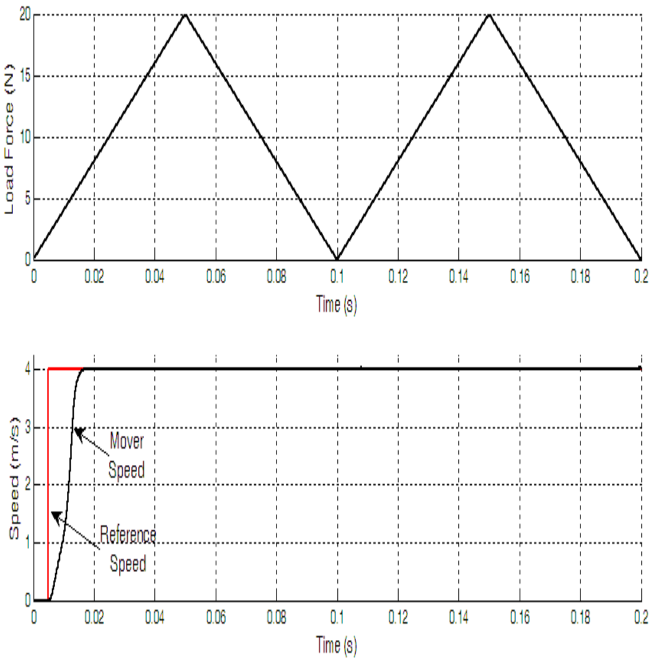

Fig. 11. Load changing effect on motor speed.

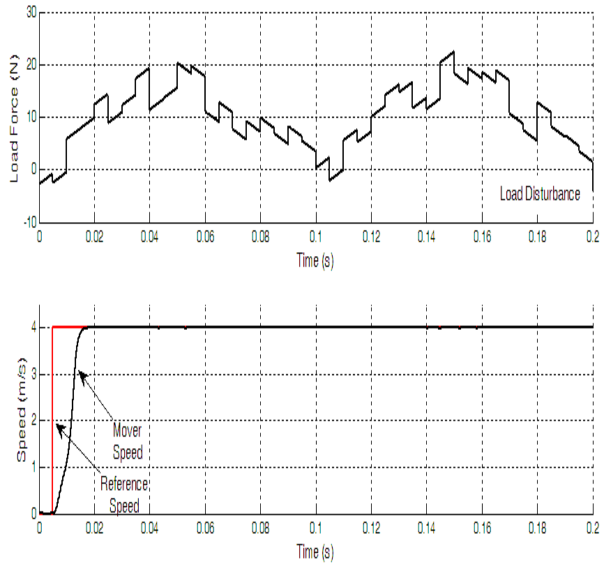

Fig. 12. Load disturbances effect on motor speed

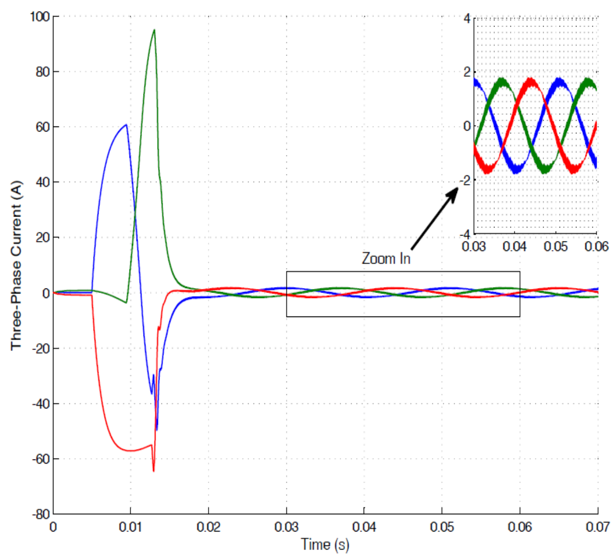

Fig. 13. Three-phase LPMSM current with 20 N load applied at t=5ms

5

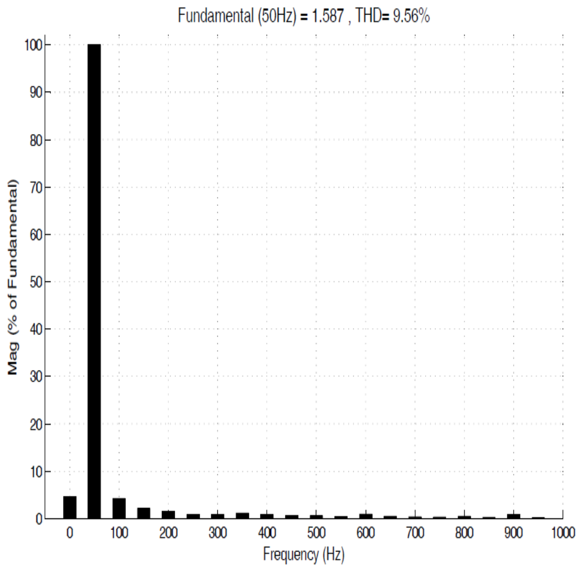

Fig. 14. Harmonic distortion diagram

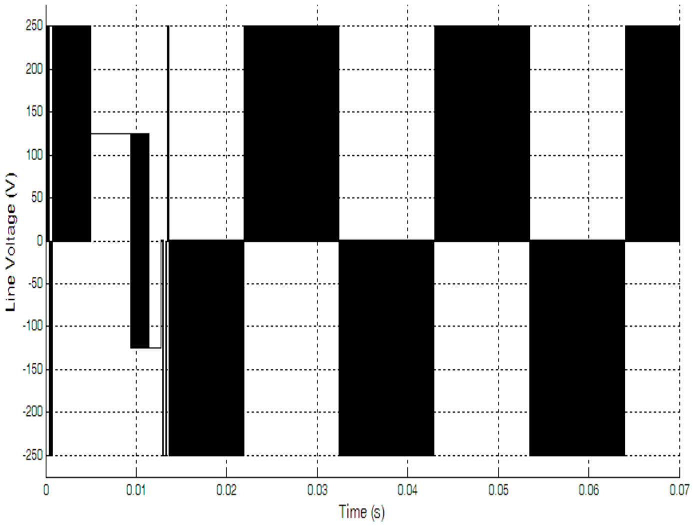

Fig. 15. Simulated line voltage waveform applying 20 N load at t=5 ms

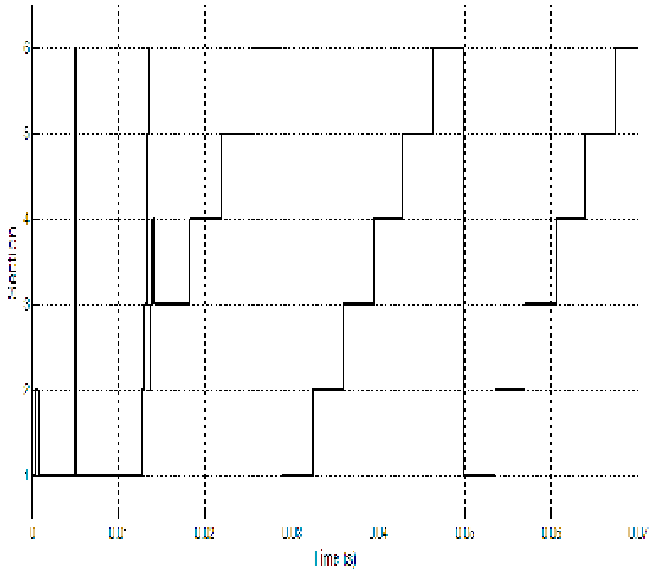
Fig. 16. Section transform of voltage vector applying 20 N load at t=5ms

maximum load conditions. In case two, previous scheme for load with disturbances is applied as shown in Fig. 12.

Simulation conditions are similar to the first case. Simulation result shows that load disturbances have no impact on the motor speed and it remains constant during simulation period. These two cases show the robustness of the designed system.

C. *Motor Current*

For a constant speed reference of 4 m/s, 20 N load is applied at t=5 ms for simulation period of 70 ms, three-phase motor current is shown in Fig. 13. As seen the startup current lasts 10 ms (from 5 to 15 ms). Three-phase currents have a good symmetry, same amplitude and with desirable sinusoidal scheme. As mentioned before, symmetrical SVM system can decrease the current THD as shown in the simulation result. According to THD diagram in Fig. 14, THD for one phase current is approximately 9.5%.

Line voltage and section variation during the simulation period have been shown in Fig. 15 and Fig. 16 respectively.

V. Conclusion

In this paper a novel control for linear permanent magnet synchronous motor drive system was designed based on symmetrical space vector modulation and current control. It was shown that the system is able to minimize the THD content in motor current and prepare a robust control system against load changing and disturbances with high quality speed tracking. The switching algorithm of symmetrical modulation was determined. Simulation results met the expected results. They showed that the system has a high quality speed tracking for constant speed and variable speed references. Motor startup time is desirable with rise time of 16 ms. The steady-state error was zero in all conditions. It was shown that the motor can move in both directions with sinusoidal speed references as an accelerated motion without any steady-state error. Also simulation results show that in load changing and disturbances conditions there is no variation in motor speed, so the system is robust. The THD of the current was approximately 9.5% which is desirable and in many applications the system does not require any filter.

The designed system is now ready for software and hardware implementation.

Acknowledgment

The authors appreciate a partial financial support from Iran National Elites Foundation (INEF).

References

[1] S. U. Chung, J. W. Kim, B. C. Woo, D. K. Hong, J. Y. Lee, and D.H. Koo, "Force ripple and magnetic unbalance reduction design for doubly salient permanent magnet linear synchronous motor", IEEE Trans. on Magnetics, Vol. 47, No. 10, pp. 4207-4210, Oct. 2011.

[2] J. Faiz, M. Manoochehry, and G. Shahgholian, "Performance improvement of permanent magnet linear synchronous motor drive using space vector modulated-direct thrust force control", Electrical Review, Poland, pp. 239-244, Vol. 11, No. 11, 2011.

[3] F. J. Lin, J. C. Hwang, P. H. Chou, and Y. C. Hung, "FPGA-based intelligent complementary sliding mode control for PMLSM servo drive system", IEEE Trans. on Pow. Elec., Vol. 1, No. 99, May 2010.

[4] Y. S. Huang, C. C. Sung, and Y. T. Shih, "Simulation of a robust fuzzy controller for linear synchronous motor systems", IEEE/SMC, pp. 2001-2006, 2008.

[5] Q. Hu, J. Zhang, D. Yu, and J. Cui, "Velocity control for rope-less elevator using permanent magnet linear synchronous motor with adaptive fuzzy PID", IEEE/ICAL, pp. 2361-2366, 2007.

6

[6] Y. S. Kung, M. H. Tsai, and C. S. Chen, “FPGA-based servo control IC for PMLSM drives with adaptive fuzzy control”, IEEE/ICIEA, pp.1-6, 2006.

[7] Y. S. Kung, C. C. Huang, and M. H. Tsai, “FPGA realization of an adaptive fuzzy controller for PMLSM drive”, IEEE Trans. on Ind. Elec., Vol. 56, No. 8, pp. 2923-2932, 2009.

[8] H. Lu, and M. Li, “Fuzzy PID controller design for PMLSM direct drive system”, IEEE/ICAE, pp. 41-45, 2009.

[9] Q. Hu, H. Yu, Y. Mu, F. Yao, and X. Zhang, “A novel fuzzy PID velocity control of linear elevator driven by the permanent magnet linear synchronous motor”, IEEE/ICEMS, pp. 1539-1542, 2008.

[10] C. Jiefan, W. Hui, and F. Yuo, “Fuzzy sliding mode variable structure control of linear motor”, IEEE/FSKD, pp. 112-115, 2009.

[11] F. J. Lin, P. H. Chou, and Y. C. Hung, W. M. Wang, "Field-programmable gate array-based functional link radial basis function network control for permanent magnet linear synchronous motor servo drive system", IET Elec. Pow. Appl., Vol. 4, No. 5, pp. 357-372, May 2010.

[12] C. Jiefan, W. Chengyuan, Y. Junyou, and Y. Dongbo, “Research on force and direct trust control for a permanent magnet linear synchronous linear motor”, IEEE/IECON, Vol. 3, pp. 2269-2272, 2004.

[13] K. Yoshida, and Z. Dai, ”Sensorless DTC propulsion of a 1/2-scale controlled-PM LSM vehicle with minimum energy-loss attractive-levitation", Vol. 1, pp. 54-59, 2002.

[14] C. Jiefan, W. Chengyuan, Y. Junyou, and L. Lifeng, “Analysis of direct thrust force control for permanent magnet linear synchronous motor”, IEEE/WCICA, Vol. 5, pp. 4418-4421, 2004.

[15] C. Sung, and Y. Huang, “Based on direct thrust control for linear synchronous motor systems”, IEEE Trans. on Ind. Elec., Vol. 56, No. 5, pp. 1629-1639, May 2009.

[16] G. Lirong, Y. Junyou, and C. Jiefan, “Direct thrust control approach using adaptive variable structure for permanent magnet linear synchronous motor”, IEEE/ICCA, pp. 2217-2220, 2007.

[17] H. Li, and Q. Wang, “Sliding mode controller based on fuzzy neural network optimization for direct torque controlled PMSM”, IEEE/WCICA, pp. 2434-2438, 2010.

[18] H. Liu and H. Cheng, “Thrust for permanent magnet synchronous motors”, Applied Mathematics and Information Sciences, Vol. 9, No. 2, pp. 927-933, 2015.

[19] M. Wang and D. Pan, “Detent force compensation for permanent magnet synchronous systems based-on structural design and control method combination”, IEEE Trans. on Industrial Electronics, In Press, 2015.

[20] C. T. Liu, C. C. Hwang, P. L. Li and S. S. Hung, “Design optimization of a double-sided hybrid excited linear flux switching PM motor with low force ripple”, IEEE Trans. on Magnetics, Vol. 50, No. 11, 8102704, Nov. 2014.

[21] Z. G. Wang, J. X. Jin, Y. G. Guo, and J. G. Zho, “SVPWM techniques and applications in HTS PMSM machines control”, Jou. of Elec. and Sci. Tec. of China, Vol. 6, No. 2, pp. 191-197, June 2008.

[22] D. O. Neacsu, “Space vector modulation - An introduction”, IEEE/IECON, pp.1583-1592, 2001.

[23] M. Zelechowski, “Space vector modulated-direct torque controlled (DTC-SVM) inverter-fed induction motor drive”, Ph.D. Thesis, Warsaw University of Technology, 2005.

[24] V. H. Prasad, “Analysis and comparison of space vector modulation schemes for three-leg and four-leg voltage source inverters”, MS Thesis, Virginia Polytechnic Institute and State University, May 1995.

[25] F. Gieras, and Z. J. Piech, “Linear synchronous motors: transportation and automation systems”, CRC Press, 1999.

[26] P. Ponomarev, “Control of permanent magnet linear synchronous motor in motion application”, M.Sc. Thesis, Lappeenranta University of Technology, 2009.

[27] N. Mohan, and T. M. Undeland, W. P. Robbins, “Power electronics, applications and design”, John Willy & Sons, Inc., 2003.

7